Signal enhancement in laser ablation ICP-MS by addition of nitrogen in the central channel gas

Zhaochu Hu,[ab] Shan Gao,*[ab] Yongsheng Liu,[a] Shenghong Hu,[a] Haihong Chen[a] and Honglin Yuan[b]

Received 19th March 2008, Accepted 4th June 2008
First published as an Advance Article on the web 8th July 2008
DOI: 10.1039/b804760j

The effects of adding nitrogen to the central gas flow (Ar + He) of an Ar plasma in laser ablation inductively coupled plasma mass spectrometry are presented. The optimum central gas flow rate was found to be negatively correlated with the N_2 gas flow rate. The addition of 5–10 ml min^{-1} nitrogen to the central channel gas in LA-ICP-MS increases the sensitivity for most of the 65 investigated elements by a factor of 2–3. The degree of enhancement depends, to some extent, on the 1st ionization energy. Another important advantage of N_2 mixed gas plasma for LA-ICP-MS is that the oxide ratios (ThO^+/Th^+) are significantly reduced (one order of magnitude). The hydride ratio (ArH^+/Ar^+) is also reduced up to a factor of 3, whereas the doubly charged ion ratio (Ca^{2+}/Ca^+) is increased. The background signals at masses 29, 31, 42, 51, 52 and 55 are significantly increased due to the nitrogen based polyatomic interferences. Compared to the spatial profiles of the ion distributions in the normal mode (without nitrogen), the addition of 5 ml min^{-1} nitrogen leads to significant wider axial profiles and more uniform distribution of ions with different physical and chemical properties. Our results also show that the makeup gas flow (central channel gas) rate has a significant effect on the ion distribution of elements with different physical and chemical properties. A very consistent increase of argon signal by the addition of nitrogen (5 ml min^{-1}) corroborates better energy transfer effect of nitrogen in the plasma.

Introduction

In the endless quest to enhance analytical capabilities, additional gases (*e.g.*, N_2, He, O_2, H_2, methane, ethene) other than argon that bleed into or replace one of the three gas flows of ICP have been extensively studied since the beginning of ICP as an ionization source.[1–10] Nitrogen is one of the most widely used molecular gases in ICP-MS, and has been utilized mainly for the attenuation of polyatomic interferences and matrix effects, and the improvement of the sensitivity and stability.[11–28] Evans and Ebdon[11,12] reduced interference from $ArCl^+$ and $ArAr^+$ on As and Se by introducing a small amount of N_2 or O_2 into the Ar plasma *via* the nebulizer gas. Using this technique, Branch *et al.*[13] successfully determined As in real sample solutions containing greater than 1% of chloride. Addition of 1% N_2 to the coolant Ar gas dramatically reduced $ArCl^+$ and ClO^+ interferences and without losing sensitivity for analyte.[14] Addition of 3% N_2 to the central channel gas flow has the same effect on polyatomic ions but causing a decrease in analyte sensitivities.[14] However, no significant effects on oxides (TiO^+, CeO^+, UO^+) and doubly charged ($^{138}Ba^{2+}$) ions were observed with or without N_2 addition.[14] Beauchemin and Craig[15] reported a reduction in sensitivity but improved detection limits owing to improved plasma stability when a sheathing gas (Ar, N_2, or H_2) was added around the aerosol coming out of the spray chamber. They also claimed improved accuracy and precision for $^{57}Fe^+/^{56}Fe^+$ and $^{76}Se^+/^{78}Se^+$ isotopic ratios even in the presence of up to 0.1 mol dm^{-3} Na by the addition of N_2 to the plasma gas.[16] Both mass discrimination and matrix effect were also found to be significantly reduced by the addition of 2–10% N_2 in the outer gas of an Ar plasma.[17,18] Lam and Horlick[19] found that nitrogen addition to the coolant gas attenuated polyatomic interferences (MO^+, ArO^+, $ArOH^+$, $ArAr^+$, ClO^+, and $ArCl^+$) by an order of magnitude and enhanced analyte signals up to a factor of 4. The degree of signal enhancement rate was found to be correlated with the metal oxide bond energy and also, to some extent, with the first ionization potential of the analyte element. Lam and McLaren[20] investigated the use of nitrogen addition at 8% to the coolant gas for reduction of UO^+ and ArO^+. Hill *et al.*,[21] Laborda *et al.*[22] and Velde-Koert and Boer[23] applied simplex optimization of the operating parameters of the spectrometer in combination with the addition of nitrogen to the outer or aerosol carrier gas to reduce the polyatomic interferences. In their investigation, special attention was paid to chlorine-based and argon dimer polyatomic interferences. Louie and Soo[24] added nitrogen and hydrogen to the main argon gas inlet of an ICP-MS. Signal enhancement was found to be greater with the Ar-N_2 than the Ar-H_2 plasma. Whereas the use of an Ar-N_2 plasma was affected by interferences from polyatomic species of nitrogen, no significant increase in background signals was observed when the Ar-H_2 plasma was used. The mechanism for this enhancement is not well understood, but could be due to the higher thermal conductivity of the Ar–N_2 mixed plasma.[3,19]

The physical attributes of a nitrogen–argon plasma are very different from those of an Ar plasma. Besides a shrinkage of the whole plasma, a 30% increase in electron density was reported by

[a]*State Key Laboratory of Geological Processes and Mineral Resources, Faculty of Earth Sciences, China University of Geosciences, Wuhan, 430074, PR China. E-mail: sgao@263.net; Fax: +86 27 67885096; Tel: +86 27 65201962*
[b]*State Key Laboratory of Continental Dynamics, Department of Geology, Northwest University, Xi'an, 710069, PR China*

Choot and Horlick[1] with 10% N_2 in the outer gas. Also, Ishii *et al.*[25] reported higher axial temperatures in the mixed-plasma for 5–10% nitrogen. The plasma shrinkage effectively moved the initial radiation zone (IRZ) away from the sampling cone, thereby requiring an increase in aerosol carrier gas or a lower sampling depth.[19] The addition of 5.9% N_2 to the plasma gas changed the bell-shaped analyte radial profiles into bimodal ones, which have a similar shape to the flattened and broadened profiles of Ar^+ and argon-containing polyatomic ions.[26] This observation, together with the absence of correlation between analyte signal and ionization potential, suggests that a predominant ionization mechanism in such a mixed-gas plasma may be charge transfer from Ar^+.[26] An addition of nitrogen to the aerosol carrier gas flow resulted in a plasma resembling a cold Ar plasma, with a wider and more diffuse central channel than that found under normal operating conditions of an Ar ICP.[27] Recently, Holliday and Beauchemin[28] published a critical review about the spatial profiling of analyte signal intensities in ICP-MS.

Laser ablation-inductively coupled plasma mass spectrometry (LA-ICP-MS) has been widely used for trace element and isotope ratio determination in solids.[29–32] The capability of LA-ICP-MS has strongly improved since its introduction, particularly with the use of a shorter laser ablation wavelength[33] and pulse width[34] and the use of helium instead of argon as ablation gas.[35,36] Advantages of this approach include little sample preparation, rapid throughput, spatially-resolved analysis and reduced water-related spectral interferences in the ICP. As summarized above, the addition of nitrogen to the ICP can be beneficial for analytical purpose in solution ICP-MS. However, the elimination of water loading of the ICP may influence its thermodynamic properties such that any analytical improvements in LA-ICP-MS would be different from those obtained with solution (SN)-ICP-MS. For example, Alder *et al.*[37] found that the presence of a small amount of water could increase the ionization and excitation temperatures and electron number density in the plasma. They advocate that it is the hydrogen from water that increases the electron density. This explanation has been demonstrated by adding hydrogen into the injection flow through which a noticeable increase of temperature was observed in ICP.[38,39] Huang *et al.*[40] concluded that the water solvent effect depends on whether the hydrogen can be released without cooling the plasma, that is, whether the hydrogen enhancement or the solvent cooling dominates the solvent effect. A general trend of increasing signal enhancement factor with increasing ionization potential in the presence of water aerosol was reported by Hu in LA-ICP-MS.[41] More recently, Guillong and Heinrich[42] reported that the addition of hydrogen (4–9 ml min^{-1}) to the helium carrier gas flow in 193 nm excimer laser ablation increased the sensitivity for most of 47 investigated elements by a factor of 2–4. However, almost no sensitivity enhancement was found for nitrogen addition (1–10 ml min^{-1}) in their investigation.[42] Durrant[43] first reported that addition of about 1% v/v N_2 to the coolant flow or addition of about 12% N_2 to the cell gas increased the Ce^+ and Th^+ signal sensitivities by a factor of 2–3 and reduced CeO^+/Ce^+ and ThO^+/Th^+ ratios by a factor of 2–3 in LA-ICP-MS. Nesbitt *et al.*[44] also reported the enhanced sensitivity of heavy mass elements by about a factor of 10 (>100 amu) by an addition of small amounts of N_2 (0.4 ml min^{-1}) into the carrier gas in LA-ICP-MS, whereas the signal intensity of the low mass elements were suppressed by about a factor of 10. Iizuka and Hirata[45] reported that the elemental sensitivities for Hf, Lu and Yb increased by a factor of 2–3 when N_2 was added into the carrier gas at a rate of 4 ml min^{-1}. This N_2 mixing technique was successfully used to improve the precision and accuracy for *in-situ* Hf isotope microanalysis of zircon using LA-MC-ICPMS.

In the present study, we systematically investigated the effects and limitations of small amounts of nitrogen mixed to the central channel gas flow of LA-ICP-MS. ICP parameters as well as interferences for multi-element capabilities are studied in detail. In an attempt to gain information on the mechanisms that are involved in the improvement of signal sensitivity, spatial profiling of ion distributions in Ar-He plasmas were also made in the presence or absence of nitrogen.

Experimental

Instrumentation

Experiments were carried out using an Agilent 7500a ICP-MS instrument (Agilent Technologies Japan) in combination with an excimer 193 nm laser ablation system (GeoLas 2005, Lambda Physik, Göttingen, Germany). All LA-ICP-MS measurements were carried out using time resolved analysis in fast, peak jumping mode. Details of the instrumental operating conditions and measurement parameters are summarized in Table 1. Helium was used as carrier gas through the ablation cell and was merged with argon (makeup gas) behind the ablation cell. The carrier and make-up gas flows were optimized to obtain maximum signal intensity for $^{139}La^+$, while keeping the ThO^+/Th^+ ratio below 0.5% and the U^+/Th^+ ratio close to 1 (NIST SRM 610). The sampling depth was fixed at 5 mm. "Sampling depth" here refers to the value set in the instrument control software, which is approximately 5 mm less than the actual distance between the end of the load coil and the sampler orifice (*i.e.* height above load coil, HALC). In order to eliminate the possible effect on ablation processes, we use a simple Y junction downstream from the sample cell to add small amounts of nitrogen to the argon

Table 1 Summary of the operating conditions used for LA-ICP-MS measurements

GeoLas 2005 laser ablation system	
Wavelength	193 nm, Excimer laser
Pulse length	15 ns
Energy density	12 J cm^{-2}
Spot size	32 μm
Laser frequency	8 Hz
Ablation cell gas	Helium (0.60 l min^{-1})
Makeup gas	Argon (0.30–1.3 l min^{-1})
Agilent 7500a ICP-MS	
rf power	950, 1150, 1350 W
Plasma gas flow rate	14.0 l min^{-1}
Auxiliary gas flow rate	1.0 l min^{-1}
Sampling depth	3, 4, 5, 7, 10 mm
Horizontal position	0, ±0.2, ±0.4, ±0.6, ±0.8, ±1.0, ±1.2, ±1.4 mm
Sampler	1 mm Ni
Skimmer	0.4 mm Ni
Ion optic settings	Typical
Dwell time per isotope	10 ms
Detector mode	Dual

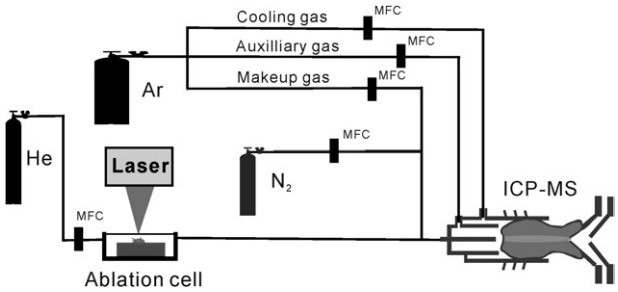

Fig. 1 Schematic set-up of the laser ablation ICP-MS system for the addition of small amounts of nitrogen. MFC denotes mass flow controller.

makeup gas flow (Fig. 1). The additional gas flow is controlled by a mass flow controller (MKS Instruments, USA) with a range up to 20 ml min^{-1}. Prior to the acquisition of ICP-MS signal, the additional gas flow is increased to the desired value over about 2 min. The ion distribution profiles were acquired by scanning the ICP torch horizontally between −1.4 mm and +1.4 mm across the sampler orifice (Table 1). Movement was performed using the software controlled motorized translation stage of the ICP-MS. The vertical profiles were recorded at five different sampling depths, between 3 mm and 10 mm according to the instrument control. All data were acquired on NIST SRM 610 glass in single spot ablation mode. Each measurement consisted of 30 s acquisition of the background signal followed by 40 s ablation signal acquisition. All data were calculated from background corrected intensities.

Results and discussion

Effect on sensitivity

The normalized signal intensity of La as a function of N_2 addition is illustrated in Fig. 2. It can be seen that increasing nitrogen addition from 1 ml min^{-1} to 5 ml min^{-1} leads to a gradual increase in normalized signal intensity. However, the maximum signal enhancement factor for La was only about 1.3 by the addition of 1–10 ml min^{-1} nitrogen under our given instrument conditions. It has been noted that the central gas flow rate must be reduced to maximize the signal when N_2 is present in the

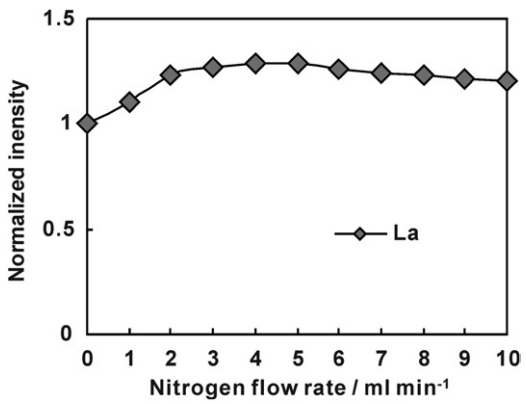

Fig. 2 The sensitivity of La as a function of N_2 addition relative to pure He + Ar flow at an rf power of 1350 W and makeup gas flow rate of 1.0 l min^{-1}.

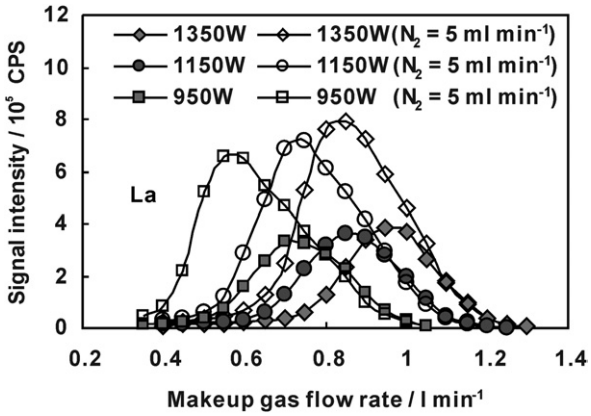

Fig. 3 Effect of varying rf powers and makeup gas (central channel gas) flow rates on the signal intensity of La in both the normal and nitrogen (5 ml min^{-1}) modes.

central gas of ICP-MS.[19] Fig. 3 illustrates the signal intensity of La as a function of makeup gas flow rate at rf powers of 950 W, 1150 W and 1350 W in both the normal and nitrogen (5 ml min^{-1}) modes. The optimum makeup gas flow rates (corresponding to the maximum signal intensity) of La in the nitrogen mode (5 ml min^{-1}) were all shifted to a lower makeup gas flow rate by about 0.15–0.20 l min^{-1} relative to those applied for the normal mode, and an enhancement factor of 2 was obtained at all rf power settings. The optimum makeup gas flow rate was found to be negatively correlated with the N_2 gas flow rate (Fig. 4). To show the possible enhancement for multi-element analysis, 65 elements were measured at different rf powers and their corresponding optimum makeup gas flow rates in both normal and nitrogen modes for comparison. The sensitivity enhancement factor for the nitrogen mode compared to the normal mode is shown in Fig. 5. Most elements have an enhancement factor of 2–3. Sulfur, arsenic and iodine have an enhancement factor of 3–4. Most of the easily ionized elements have an enhancement factor between 1.2 and 2 (*e.g.* Li, Na, K). The signal enhancement factors are in accordance with the published data for Ce and Th (up to a factor of 3) by Durrant[43] and for Hf, Lu and Yb (up to a factor of 3) by Iizuka and Hirata.[45] Unlike hydrogen and methane, no obvious sensitivity enhancement was found for nitrogen addition

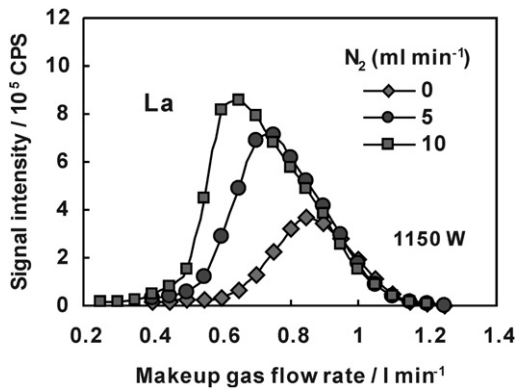

Fig. 4 Signal intensity of La as a function of makeup gas (central channel gas) flow rate in the presence of 0, 5 and 10 ml min^{-1} N_2 flow, respectively.

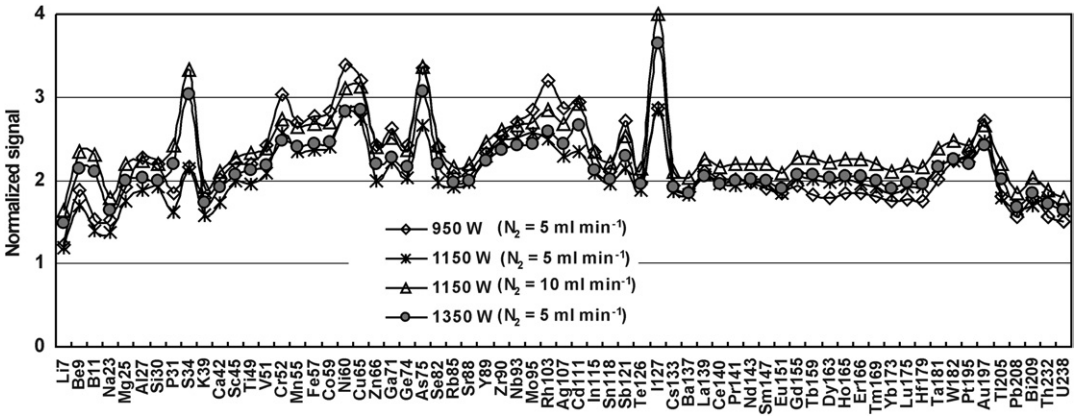

Fig. 5 Sensitivity enhancement factors for 65 elements in the presence of 5 and 10 ml min^{-1} N_2 relative to the normal mode (He + Ar) at different rf powers and their corresponding optimum makeup gas flow rates.

(1–10 ml min^{-1}) in LA-ICP-MS by Guillong and Heinrich.[42] Only slight increase for selected elements like arsenic (enhancement factor 1.3) and gold (1.5) was observed, but sensitivities of other elements decreased with increasing nitrogen flow. Since they acquired their data at the same central gas flow rate, change in optimum central gas flow rate due to the addition of N_2 is probably the main reason why they, using nitrogen as the additional gas in LA-ICP-MS, have not found the same signal enhancement as has been documented in this work and references.[43,45] Fig. 6 illustrates the relation between the signal enhancement factor and the first ionization potential for the 65 elements. There is a roughly increasing trend of signal enhancement factor with increasing ionization potential. However, the significant scatter shows that this is not the only controlling parameter. The greater enhancement for elements with higher 1st ionization energy can be interpreted as an indicator of a higher electron temperature. Whereas, the thermal conductivity of the involved gases nitrogen, helium, and argon (N_2: 24.75, He: 151.3, Ar: 17.95 mW m^{-1} K^{-1} at 300 K) does not explain the increased heat transfer to improve the ionization efficiency. Charge transfer from NO^+ (IP = 9.26 eV) to M has been proposed to explain the sensitivity enhancements of the hard-to-ionize analytes in nitrogen–argon mixed gas ICP.[2,19] This charge transfer reaction requires that the ionization potential of the NO exceeds the value of M. As a result, the NO^+–analyte atom charge transfer reaction hypothesis is not applicable to the signal enhancement of elements whose ionization potential is higher than that of NO (*e.g.*, As, Se, S, I). Since no water solvent is present in LA-ICP-MS (water contains a high proportion of oxygen), the amount of NO^+ is also expected to be very small. It has been noted that N_2 has a thermal conductivity, which is higher than that of argon by a factor of 32 at 7000 K.[43,46] It is therefore possible that the increased sensitivity enhancements result from the increased thermal conductivity. A similar but slighty stronger enhancement effect (for most of the 47 investigated elements by a factor of 2–4) was found for the addition of hydrogen (4–9 ml min^{-1}) in LA-ICP-MS by Guillong and Heinrich.[42] This H_2 mixing technique is of immediate benefit for many applications. However, the simple N_2 mixing technique described here has the potential advantage of easier handling and different kinds of interferences.

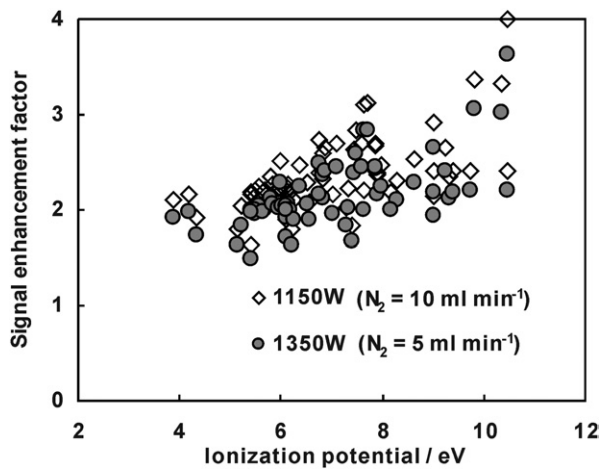

Fig. 6 Correlation of the 1st ionization energy and the sensitivity enhancement factor for nitrogen addition.

Several applications can benefit from the nitrogen addition. The simultaneous determinations of U–Pb age, Hf isotopes and trace element compositions of zircon by excimer laser ablation quadrupole and multiple collector ICP–MS is now done routinely in our laboratory.[47] To obtain further improvements in precision of the trace element and isotopic data from zircon material with a small ablation pit size, enhancement of the elemental sensitivity of the LA-MC-ICP-MS/LA-ICP-MS instrument was highly required. Other applications such as the determination of crystal-melt trace element partition coefficient,[48] where improved limits of detection or an increased spatial resolution is of importance, are possible candidates to benefit from the nitrogen mode in LA-ICP-MS.

Effect on background and interferences

Although instrumental sensitivity affects the analytical capabilities of ICP-MS, instrumental background signals at respective masses have at least equal importance. It is expected that nitride formation is a problem for some elements by the presence of nitrogen in the plasma. Average gas blank intensities for the normal mode and the nitrogen mode (N_2 = 5 ml min^{-1}) at rf powers of 1350 W and 1150 W are shown in Fig. 7. The makeup

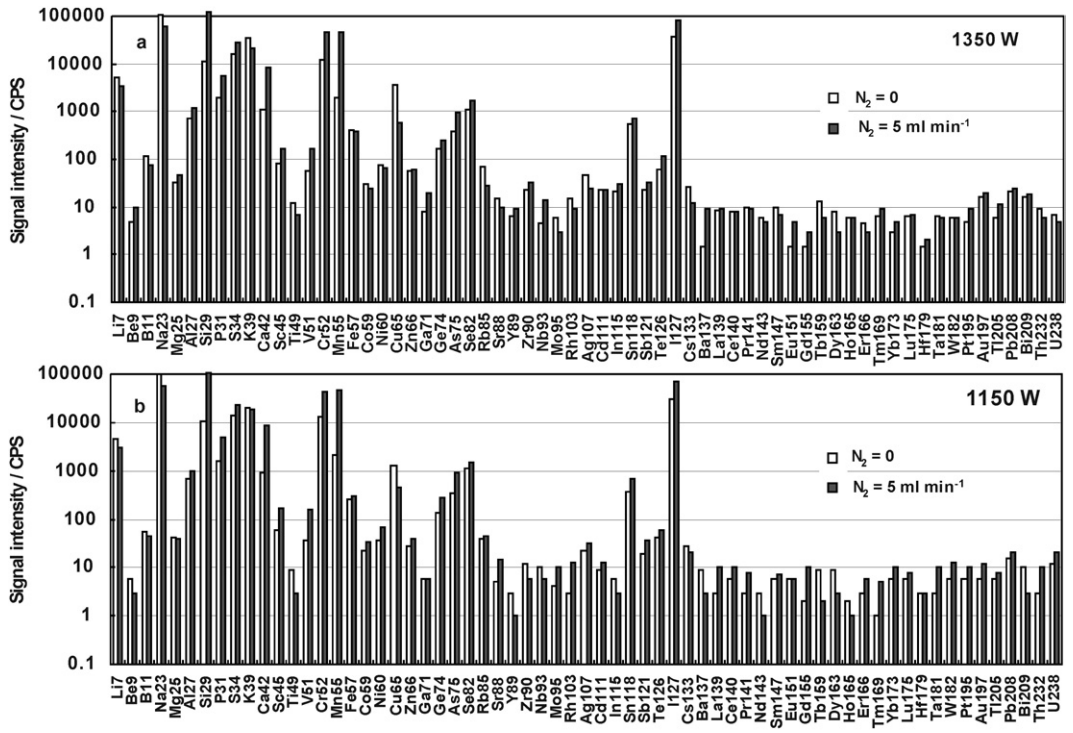

Fig. 7 Average gas blank intensities for the normal and nitrogen modes at rf powers of (a) 1350 W and (b) 1150 W and their corresponding optimum makeup gas flow rate.

gas flow rates were adjusted to the optimum values in both normal and nitrogen modes, respectively. Higher gas blank intensities can be found especially on $^{29}Si^+$ from $^{14}N^{14}N^1H^+$ and $^{14}N^{15}N^+$, on $^{31}P^+$ from$^{15}N^{16}O^+$, $^{14}N^{16}O^1H^+$ and $^{15}N^{15}N^1H^+$, on $^{42}Ca^+$ from $^{14}N^{14}N^{14}N^+$ and $^{12}C^{14}N^{16}O^+$, on ^{51}V from $^{36}Ar^{15}N^+$ and $^{36}Ar^{14}N^1H^+$, on $^{52}Cr^+$ from $^{38}Ar^{14}N^+$ and $^{36}Ar^{15}N^1H^+$, and on $^{55}Mn^+$ from $^{40}Ar^{14}N^1H^+$ and $^{40}Ar^{15}N^+$. These interferences were not identified but are proposed as the most likely ones. Elements whose background signals higher than 10 CPS usually have an increased gas blank by the similar factor as the sensitivity increase of the signal. The gas blank of these elements is dominated by contamination of the elements. Elements (*e.g.*, REE) with gas blanks less than 10 CPS that are mainly dominated by the dark counts have very similar gas blank intensities for both modes.

It is also likely that the formation of molecular ions from nitrogen with elements present in the sample analyzed may cause additional interferences. We thus analyzed zircon ($ZrSiO_4$) standard GJ-1 and pure copper (Cu). The yield of $^{90}Zr^{14}N^+/^{90}Zr^+$ is 0.00032% and 0.00062% in the presence of 5 ml min^{-1} and 10 ml min^{-1} of nitrogen at a fixed power of 1350 W and their corresponding optimum makeup gas flow rate, respectively. The yield of $^{63}Cu^{14}N^+/^{63}Cu^+$ is 0.000048% and 0.000088% in the presence of 5 ml min^{-1} and 10 ml min^{-1} of nitrogen, respectively. Thus, the interferences of molecular ions from nitrogen with elements present in the sample analyzed are usually negligible.

Effect on oxides

Oxides represent one important concern for trace metal analyses in ICP-MS techniques. For analysis of geological materials potentially troublesome examples include the interference of Ba and light rare earth elements (LREE) oxides on middle rare earth elements (MREE) as well as MREE oxides on heavy rare earth elements (HREE), and HREE oxides on Re. In LA-ICP-MS, as sample material cannot be chemically treated prior to analysis to remove specific troublesome elements, oxides may be of particular concern. Kent and Ungerer[49] confirm that oxide production in LA-ICP-MS is related to the strength of the M–O bond in the MO^+ ion, and in agreement with solution-based measurements and theoretical considerations, M–O bond strength correlates linearly with $\log(MO^+/M^+)$. Monitoring the ThO^+/Th^+ ratio is particularly useful for LA-ICP-MS as there is no naturally occurring isotope at the ThO^+ mass (248), and the Th–O bond is among the strongest known for oxides (878.9 KJ mol^{-1}) and thus ThO^+/Th^+ production rates should also represent the maximum oxide production rate expected for a given set of plasma conditions. Fig. 8 shows the ThO^+/Th^+ ratio as a function of makeup gas flow rate in both normal and nitrogen modes (5 ml min^{-1}) at (a) 1350 W and (b) 1150 W [The dashed lines show the difference (0.15–0.20 l min^{-1}) of optimum makeup gas flow rates for normal and nitrogen (5 ml min^{-1}) modes, which yield the maximum signal intensity of Th^+]. Under the corresponding optimum makeup gas flow rate, the ThO^+/Th^+ ratio decreased from about 0.2% in the normal mode to about 0.02% in the nitrogen mode (Fig. 8). The lower oxide ratio may indicate higher gas temperature, and which could result in decomposition of MO. However, the significantly increased NO^+ signal in nitrogen mode suggests that removal of oxygen through NO formation is the dominating reason for the reduction of the oxide ratio (Fig. 9). Compared to the H_2 mixing technique,[42] the significantly

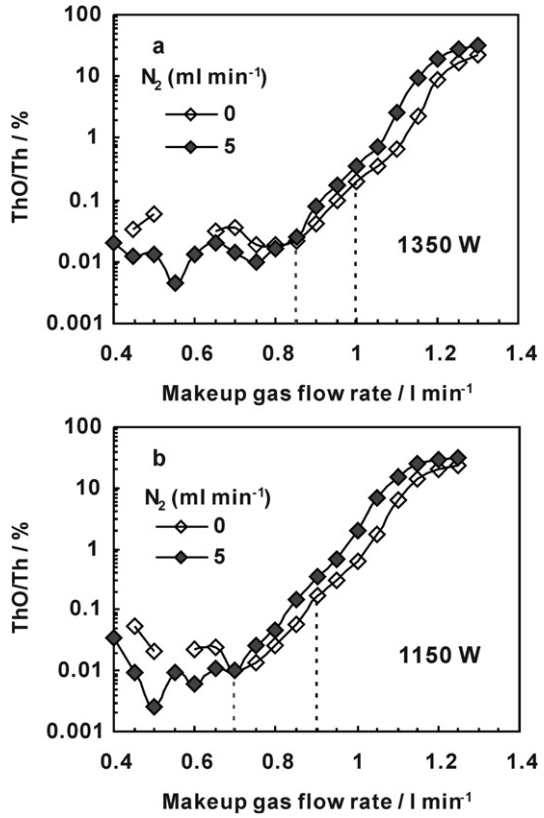

Fig. 8 Effect of makeup gas flow rate on ThO^+/Th^+ ratio at rf powers of (a) 1350 W and (b) 1150 W for the normal and nitrogen (5 ml min^{-1}) modes. The dashed lines show the difference (0.15–0.20 l min^{-1}) of optimum makeup gas flow rates for the normal and nitrogen (5 ml min^{-1}) modes, which yield the maximum signal intensity of Th^+.

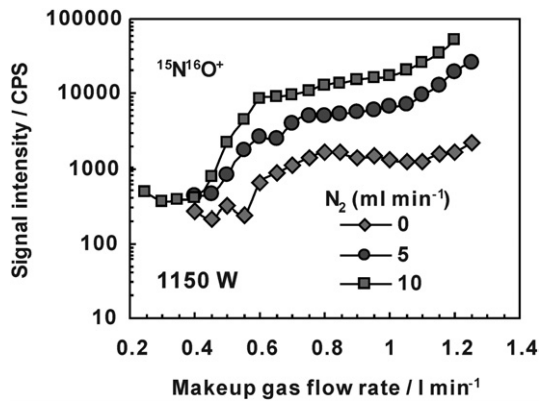

Fig. 9 Effect of makeup gas flow rate on $^{15}N^{16}O^+$ signal at an rf power of 1150 W for the normal and nitrogen modes.

reduced oxide formation is the major advantage of the N_2 mixing technique.

Effect on hydride and doubly charged ions

Hydride (MH^+) and doubly charged (M^{2+}) ions are other classical interferences in ICP-MS. In this investigation, ArH^+/Ar^+ is used to represent the hydride production, and $^{42}Ca^+$ is selected to

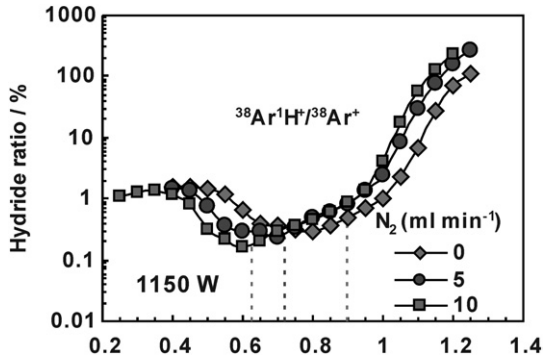

Fig. 10 Effect of makeup gas flow rate on $^{38}Ar^1H^+/^{38}Ar^+$ ratio at an rf power of 1150 W for the normal and nitrogen modes. The dashed lines show the difference (0.2–0.30 l min^{-1}) of optimum makeup gas flow rates for normal and nitrogen (5–10 ml min^{-1}) modes, which yield the maximum signal intensity of K^+.

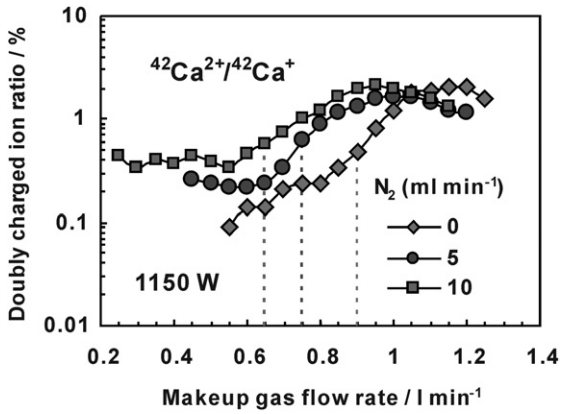

Fig. 11 Effect of makeup gas flow rate on $^{42}Ca^{2+}/^{42}Ca^+$ at an rf power of 1150 W for the normal and nitrogen modes. The dashed lines show the difference (0.20–0.30 l min^{-1}) of optimum makeup gas flow rates for normal and nitrogen (5–10 ml min^{-1}) modes, which yield the maximum signal intensity of $^{42}Ca^+$.

study the yield of doubly charged ions since ^{21}Ne is not present in the NIST SRM 610 and almost not ionized in the plasma due to its high first ionization potential (21.56 eV). As shown in Fig. 10, the ArH^+/Ar^+ formation decreases from 0.50% in the normal mode to about 0.17% in the nitrogen mode (10 ml min^{-1}) at their corresponding optimum carrier gas flow rate. The reduced hydride ratio may be due to the competition reaction of H with nitrogen. In contrast, the doubly-charged ratio (Ca^{2+}/Ca^+) increased from 0.47% in the normal mode to 0.63% in the nitrogen mode (Fig. 11). The higher doubly-charged ratio can also be interpreted as an indication for a higher electron temperature in the plasma when nitrogen is present. It is therefore important to note that the increased doubly-charged ratio can become a problem with applications where elements with low 2nd ionization energy are involved (*e.g.*, Ca, Ba, REE).

Effect on spatial profiles of the ion distributions

Laser ablation is known to produce a complex aerosol with different particle sizes[50] and particle size dependent elemental

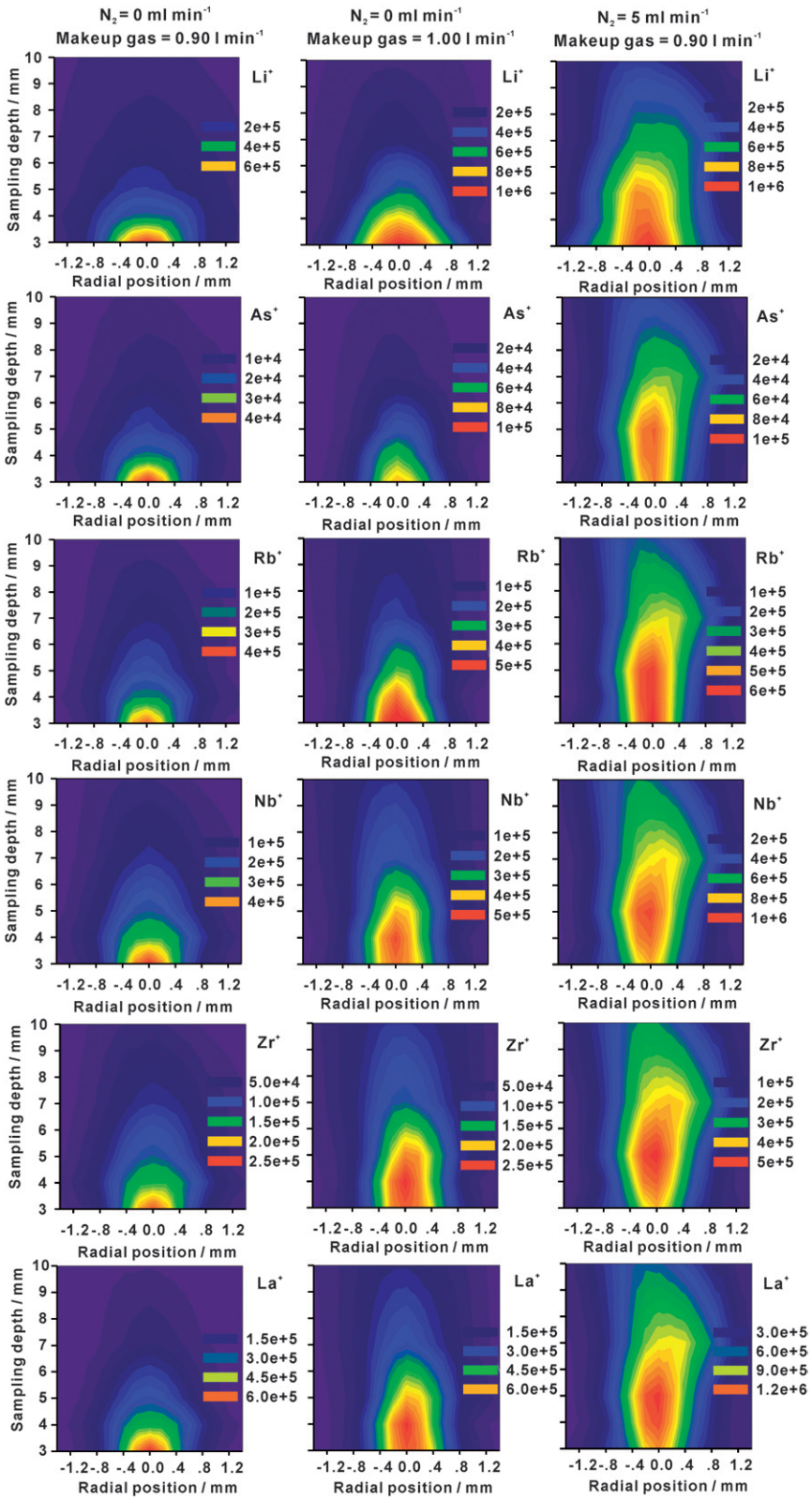

Fig. 12 Radial and axial intensity distributions for selected elements at an rf power of 1350 W in the normal (makeup gas flow rates: 0.90 l min^{-1} and 1.0 l min^{-1}) and nitrogen (makeup gas flow rate: 0.90 l min^{-1}; N_2 = 5 ml min^{-1}) modes.

composition[51,52] and therefore leads to a complex interaction of these particles with the ICP.[53] The distribution of ions within the ICP provides useful information about the treatment of the aerosol inside the ion source and the history of the analyte ion before sampling by the vacuum interface, and valuable insight into the predominant ionization mechanism(s).[28,53] MacEdone *et al.*[54] have recently shown that the signal intensities measured by scanning the ICP across the sampler orifice do actually represent the distribution of ions within the ICP. It should be noted, however, that the measured ion signals most probably do not represent the absolute number densities within the ICP.[53] Especially the presence of the vacuum interface in contact with the ICP may alter the ion and electron number densities for different radial and axial sampling positions differently.[55] More recently, Wang *et al.*[53] have made an excellent study about the dependence of the radial and axial ion distributions in the ICP for aerosols generated from silicate samples at different laser ablation conditions (wavelength, pulse duration, carrier gas). In the present study, we focused on the effect of small amounts of N_2 mixed to the central channel gas (Ar + He) on the spatial profiles of the ion distributions. Fig. 12 shows the ion distributions of selected elements with different physical and chemical properties in both normal and nitrogen modes. The spatial profiles of the ion distributions are non-symmetric especially at the higher sampling depth in the nitrogen mode. This may be caused by a distortion of the symmetry of the ICP through the torch box exhaust system which is arranged so that the gas flow is dragged towards the negative positions of the torch. It has been reported that the dependence of ion distributions on atomic mass is reduced and the profiles for easily vaporized and refractory elements (^{85}Rb *vs.* ^{93}Nb) are almost identical, while the dependence on ionization energy remains significant when helium is used as carrier gas, which is a result of faster vaporization of the aerosol and higher mobility of vapor and ions when helium is present in the central channel of the ICP.[53] Our results show that the makeup gas flow rate (central channel gas) has a significant effect on the ion distribution of elements with different physical and chemical properties. All elements' axial width increased significantly with increasing makeup gas flow rate (Fig. 12). At the high makeup gas flow rate (1.0 l min^{-1}), the profile difference for easily vaporized and refractory elements ($^{85}Rb^+$ *vs.* $^{90}Nb^+$, $^{93}Zr^+$ and $^{139}La^+$) are very small. However, high first ionization element $^{75}As^+$ (9.81 eV) shows a remarkably faster decay relative to the easily ionized element $^{85}Rb^+$ (4.18 eV) with increasing sampling depth. The increased makeup gas flow rate is thought to lead to a cooling effect in the plasma. As show in Fig. 13, the signal intensities of Ar^+ are significantly reduced by the increase of makeup gas from 0.90 l min^{-1} to 1.0 l min^{-1}. The very high first ionization potential of Ar makes it very sensitive to the variation of temperature in plasma. The rapid decay of $^{75}As^+$ signal with increasing sampling depth is thus attributed to the neutralization, which is most pronounced for ions with high ionization energies especially at high makeup gas flow rate. On the contrary, $^{93}Nb^+$, $^{90}Zr^+$ and $^{139}La^+$ show obviously wider axial distributions than easily vaporized element $^{85}Rb^+$ at the low makeup gas flow rate (0.90 l min^{-1}), whereas, the profile difference for different ionization energy elements (^{85}Rb vs. ^{75}As) is very small. The axial ion distribution is expected to be a convolution between radial diffusion and vaporization of the aerosol particles following the flow of the carrier gas inside the central channel of the ICP.[53] Atoms and ions have the greatest mobility and thus can move further away from the axis of the ICP, while particles should generally follow the streamlines of the carrier gas when entering the central channel.[56,57] Elements like Nb, Zr and La, which are less efficiently vaporized in the aerosol particle, are supposed to survive longer in the plasma, and thus can move further away along the axis of the ICP. The reduced profile difference for different ionization energy elements should be attributed to the reduced cooling effect at the lower makeup gas rate. Compared to the spatial profiles of the ion distributions in normal mode, there is a significant wider axial profile and more uniform distribution of ions in the nitrogen mode (Fig. 12). Not only the profile difference for easily vaporized and refractory elements ($^{85}Rb^+$ vs. $^{93}Nb^+$, $^{90}Zr^+$ and $^{139}La^+$) are reduced, but also the profile difference for different first ionization elements ($^{85}Rb^+$ *vs.* $^{75}As^+$) is minimized, and consequently variability in the intensity ratios for different elements is reduced. Improving argon signal intensity needs higher plasma excitation temperature owing to its high ionization potential (15.76 eV). There is a very consistent increase of argon signal in the presence of nitrogen (5 ml min^{-1}) which corroborates better energy transfer effect of nitrogen in the plasma (Fig. 13). However, the significantly changed spatial profiles of the ion distributions and increased signal intensities suggest that the addition of small amounts of N_2 affect not only the fundamental parameters and bulk properties of the plasma, but also how energy is coupled and transported through the

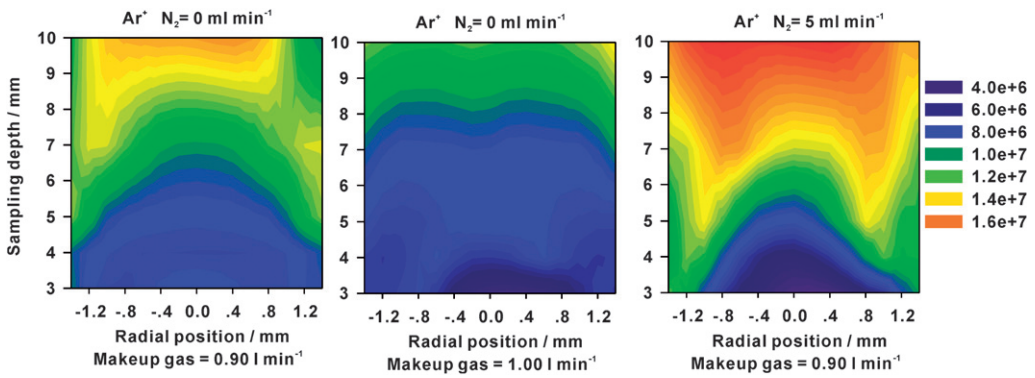

Fig. 13 Radial and axial intensity distributions for Ar^+ at an rf power of 1350 W in the normal (makeup gas flow rates: 0.90 l min^{-1} and 1.0 l min^{-1}) and nitrogen (makeup gas flow rate: 0.90 l min^{-1}; N_2 = 5 ml min^{-1}) modes.

discharge and how that energy interacts with the sample. Further investigations are needed to reveal the exact mechanism.

Conclusions

Results presented here indicate that adding small amounts of nitrogen to the central gas flow has an important role in improving the performance of LA-ICP-MS. The sensitivities for most of 65 investigated elements were increased by a factor of 2–3 while ThO^+/Th^+ ratio is reduced by one order of magnitude. Hydride ratios are also modestly reduced (up to a factor of 3). However, doubly charged ion ratios are increased. Compared to the spatial profiles of the ion distributions in normal mode (without nitrogen), a significant wider axial profile and more uniform distribution of ions with different physical and chemical properties are observed in nitrogen mode. The sensitivity enhancement and more uniform distribution of ions results partly from a higher plasma temperature, and therefore higher ionization efficiency. A very consistent increase of argon signal by the addition of nitrogen supports better energy transfer effect of nitrogen in the plasma. Because of the simplicity of the method, it will be of immediate benefit for applications where improved limits of detection or an increased spatial resolution is of importance.

Acknowledgements

This research is supported by the National Nature Science Foundation of China (Grants 40703006, 90714010, 40521001 and 40673019) and the Ministry of Education of China as well as the State Administration of the Foreign Experts Affairs of China (B07039, IRT0441, 306021, and NCET-05-0664).

References

1 E. H. Choot and G. Horlick, *Spectrochim. Acta, Part B*, 1986, **41**, 889–906.
2 R. S. Houk, A. Montaser and V. A. Fassel, *Appl. Spectrosc.*, 1983, **37**, 425–428.
3 A. Montaser and R. L. Vanhoven, *Crit. Rev. Anal. Chem.*, 1987, **18**, 45–103.
4 A. Montaser, S. K. Chan and D. W. Koppenaal, *Anal. Chem.*, 1987, **59**, 1240–1242.
5 D. Hausler, *Spectrochim. Acta, Part B*, 1987, **42**, 63–73.
6 N. N. Sesi, A. Mackenzie, K. E. Shanks, P. Y. Yang and G. M. Hieftje, *Spectrochim. Acta, Part B*, 1994, **49**, 1259–1282.
7 M. Murillo and J. M. Mermet, *Spectrochim. Acta, Part B*, 1989, **44**, 359–366.
8 K. S. Park, S. T. Kim, Y. M. Kim, Y. J Kim and W. Lee, *Bull. Korean Chem. Soc.*, 2003, **24**, 285–290.
9 I. Rodushkin, P. Nordlund, E. Engström and D. C. Baxter, *J. Anal. At. Spectrom.*, 2005, **20**, 1250–1255.
10 L. Ebdon, M. J. Ford, R. C. Hutton and S. J. Hill, *Appl. Spectrosc.*, 1994, **48**, 507–516.
11 E. H. Evans and L. Ebdon, *J. Anal. At. Spectrom.*, 1989, **4**, 299–300.
12 E. H. Evans and L. Ebdon, *J. Anal. At. Spectrom.*, 1990, **5**, 425–430.
13 S. Branch, L. Ebdon, M. Ford, M. Foulkes and P. O'Neill, *J. Anal. At. Spectrom.*, 1991, **6**, 151–154.
14 J. S. Wang, E. H. Evans and J. Caruso, *J. Anal. At. Spectrom.*, 1992, **7**, 929–936.
15 D. Beauchemin and J. M. Craig, in Plasma Source Mass Spectrometry, eds. K. E. Jarvis, A. L. Gray, J. Jarvis and J. Williams, *Special Publication No. 85*, Royal Society of Chemistry, Cambridge, 1990, p. 25.
16 D. Beauchemin and J. M. Craig, *Spectrochim. Acta, Part B*, 1991, **46**, 603–614.
17 J. M. Craig and D. Beauchemint, *J. Anal. At. Spectrom.*, 1992, **7**, 937–942.
18 G. Xiao and D. Beauchemin, *J. Anal. At. Spectrom.*, 1994, **9**, 509–518.
19 J. W. H. Lam and G. Horlick, *Spectrochim. Acta, Part B*, 1990, **45**, 1313–1325.
20 J. W. Lam and J. W. McLaren, *J. Anal. At. Spectrom.*, 1990, **5**, 419–424.
21 S. J. Hill, M. J. Ford and L. Ebdon, *J. Anal. At. Spectrom.*, 1992, **7**, 719–725.
22 F. Laborda, M. J. Baxter, H. M. Crews and J. Dennis, *J. Anal. At. Spectrom.*, 1994, **9**, 727–736.
23 T. van der Velde-Koerts and J. L. M. de Boer, *J. Anal. At. Spectrom.*, 1994, **9**, 1093–1098.
24 H. Louie and S. Y. P. Soo, *J. Anal. At. Spectrom.*, 1992, **7**, 557–564.
25 I. Ishii, D. W. Golightly and A. Montaser, *J. Anal. At. Spectrom.*, 1988, **3**, 965–968.
26 A. E. Holliday and D. Beauchemin, *J. Anal. At. Spectrom.*, 2003, **18**, 289–295.
27 A. E. Holliday and D. Beauchemin, *Can. J. Anal. Sci. Spectrosc.*, 2002, **47**, 91–97.
28 A. E. Holliday and D. Beauchemin, *Spectrochim. Acta, Part B*, 2004, **59**, 291–311.
29 S. F. Durrant, *J. Anal. At. Spectrom.*, 1999, **14**, 1385–1403.
30 R. E. Russo, X. L. Mao, H. C. Liu, J. Gonzalez and S. S. Mao, *Talanta*, 2002, **57**, 425–451.
31 D. Günther and B. Hattendorf, *Trend. Anal. Chem.*, 2005, **24**, 255–265.
32 P. J. Sylvester, *Geostand. Geoanal. Res.*, 2006, **30**, 197–207.
33 D. Günther, R. Frischknecht, C. A. Heinrich and H. J. Kahlert, *J. Anal. At. Spectrom.*, 1997, **12**, 939–944.
34 R. E. Russo, X. L. Mao, J. J. Gonzalez and S. S. Mao, *J. Anal. At. Spectrom.*, 2002, **17**, 1072–1075.
35 S. M. Eggins, L. P. J. Kinsley and J. M. G. Shelley, *Appl. Surf. Sci.*, 1998, **129**, 278–286.
36 D. Günther and C. A. Heinrich, *J. Anal. At. Spectrom.*, 1999, **14**, 1363–1368.
37 J. F. Alder, R. M. Bombelka and G. F. Kirkbright, *Spectrochim. Acta, Part B*, 1980, **35**, 163–175.
38 Y. Q. Tang and C. Trassy, *Spectrochim. Acta, Part B*, 1986, **41**, 143–150.
39 P. E. Walters and C. A. Barnardt, *Spectrochim. Acta, Part B*, 1988, **43**, 325–337.
40 M. Huang, H. Kojima, T. Shirasaki, A. Hirabayashi and H. Koizumi, *Anal. Chim. Acta*, 2000, **413**, 217–222.
41 Z. C. Hu, PhD dissertation, Northwest University, Xi'an, 2006.
42 M. Guillong and C. A. Heinrich, *J. Anal. At. Spectrom.*, 2007, **22**, 1488–1494.
43 S. F. Durrant, *Fresenius' J. Anal. Chem.*, 1994, **349**, 768–771.
44 R. W. Nesbitt, T. Hirata, I. B. Bilter and J. A. Milton, *Geostand. Newsl.*, 1997, **20**, 231–243.
45 T. Iizuka and T. Hirata, *Chem. Geol.*, 2005, **220**, 121–137.
46 S. Greenfield, I. L. Jones, H. McGreachin and P. B. Smith, *Anal. Chim. Acta*, 1975, **74**, 225–245.
47 H. L. Yuan, G. Shan, M. N. Dai, C. L. Zong,, D. Günther, G. H. Fontaine, X. M. Liu and C. R. Diwu, *Chem. Geol.*, 2007, **247**, 100–118.
48 M. Petrelli, L. Caricchi and P. Ulmer, *Geostand. Geoanal. Res.*, 2007, **31**, 13–25.
49 A. J. R. Kent and C. A. "Andy" Ungerer, *J. Anal. At. Spectrom.*, 2005, **20**, 1256–1262.
50 M. Guillong and D. Günther, *J. Anal. At. Spectrom.*, 2002, **17**, 831–837.
51 H. R. Kuhn and D. Günther, *J. Anal. At. Spectrom.*, 2004, **19**, 1158–1164.
52 Z. C. Hu, Y. S. Liu, S. Gao, S. H. Hu, R. Dietiker and D. Günther, *J. Anal. At. Spectrom.*, 2008, **23**, DOI: 10.1039/b803934h.
53 Z. K. Wang, B. Hattendorf and D. Günther, *J. Anal. At. Spectrom.*, 2006, **21**, 1143–1151.
54 J. H. MacEdone, A. A. Mills and P. B. Farnsworth, *Appl. Spectrosc.*, 2004, **58**, 463–467.
55 S. A. Lehn, K. A. Warner, M. Huang and G. M. Hieftje, *Spectrochim. Acta, Part B*, 2002, **57**, 1739–1751.
56 I. Stewart, C. E. Hensman and J. W. Olesik, *Appl. Spectrosc.*, 2000, **54**, 164–174.
57 K. Kahen, K. Jorabchi, C. Gray and A. Montaser, *Anal. Chem.*, 2004, **76**, 7194–7201.